Int. J. Electrochem. Sci., 15 **(2020)** 11401 – 11415, doi: 10.20964/2020.11.41

International Journal of
ELECTROCHEMICAL
SCIENCE
www.electrochemsci.org

Surface Properties of Nanostructured Gold Coatings Electrodeposited at Different Potentials

Mohammad Hafizudden Mohd Zaki, Yusairie Mohd and Lim Ying Chin*

Electrochemical Materials and Sensor (EMaS) Research Group, Faculty of Applied Sciences, Universiti Teknologi MARA (UiTM), 40450 Shah Alam, Selangor, Malaysia.
*E.mail: yusairie@uitm.edu.my

Received: 27 February 2020 / *Accepted:* 7 September 2020 / *Published:* 30 September 2020

Nanostructured gold coating were synthesized on the surface of screen-printed carbon electrode (SPCE) via electrodeposition technique from acidic gold solution at four different potentials (i.e.: +1.0 V, +0.48 V, -0.3 V and -0.7 V). The gold coatings were characterized by FESEM, EDAX and XRD for their morphology, elemental composition and crystallite size, respectively. The electrochemical active surface area (ECSA) and electron transfer of gold nanostructures were investigated by cyclic voltammetry (CV) analysis in 0.5 M H_2SO_4 and in 1 mM Fe $(CN)_6^{-3/-4}$ + 0.1 M KCl solution, respectively. Deposition at +1.0 V has produced gold coatings with tetrahedral like structures as imaged by FESEM. Meanwhile, deposition at +0.48 V, a coating formed was quasi-spherical and facetted crystalline structures. However, deposition at more cathodic potential (i.e.: -0.3 V) resulted in the formation of dendrite-like gold nanoclusters with several micrometres of stem structures. Large micrometres of stem and feather-like branches were formed for deposition at more negative potential of -0.7 V. The EDAX analysis showed that the nanostructured gold coating deposited at +0.48 V has the highest gold purities with elemental composition of 99.68 wt. %. The XRD analysis revealed that all nanostructured gold coatings were composed of cubic crystallite structures where the highest crystallite size of 93.18 nm was obtained for deposition at -0.7 V. Furthermore, the coating deposited at -0.7 V also has the highest ECSA value of 3.851 cm^2 as well as the highest oxidation and reduction current peak for Fe $(CN)_6^{-3/-4}$ reaction which demonstrated the best electron transfer by CV. The electrochemical kinetic mechanism on its surface is predominantly controlled by a linear diffusion.

Keywords: Gold nanostructures; Electrodeposition; Cyclic voltammetry; Chronoamperometry; Deposition potential

1. INTRODUCTION

In recent years, extensive studies have been devoted to surface modification of materials with nanostructures due to their potential applications in fuel cells, biosensors, photonic materials and others

[1-3]. Nanostructured materials have attracted a considerable deal of attention because of their unique optical, electronic, catalytic, magnetic properties, enhanced electrochemical surface area and mass transport which could be easily introduced into devices via the nanostructure's attachment [2]. Recently, preparation and potential applications of noble metal gold nanostructures have been attentively investigated by researchers due to their excellent physical and chemical properties such as large surface area-to-volume ratio, excellent electron kinetics, unique optical and electronic properties and can be functionalized easily for the adsorption of various biomolecules [4-10]. The presence of these properties can improve the electrode performance through fast electron-transfer kinetics and decrease overpotentials for electrochemical reaction [11,12].

Conventionally, bulk gold metal electrode has been widely used for electrocatalytic activity and biocompatibility studies [5]. However, such type of electrode is not preferable in practical application due to its high cost, thus minimization of the cost of this precious metal needs to be considered. Besides that, this bulk gold metal electrode has low surface area due to flat surface leading to low catalytic performance in electrochemical reaction [13]. Gold nanostructures have larger specific surface area-to-volume ratio as compared to the bulk counterpart [14,15]. Therefore, in this study, gold nanostructures coating is deposited onto a relatively low-cost screen-printed carbon electrode (SPCE) as the substrate in order to minimize the cost of producing gold electrodes.

Electrodeposition is one of the techniques that can be used to deposit gold nanostructures on the cheap and inactive but conductive electrode surface such as SPCE. The technique is a well-known conventional surface modification method to improve the surface characteristics, decorative and functional of a wide variety of materials. Nowadays, electrodeposition has emerged as an accepted versatile technique for the preparation of nanostructured electrodes [14,16]. However, the electrodeposition conditions like deposition potential, current density and deposition time need to be properly controlled in order to produce a highly active surface area of gold electrode with improved electrocatalytic performance. The gold nanostructures prepared at different deposition conditions with different surface properties can behave differently for various catalytic performances [16]. Besides, the interplay between the crystal growth rate and mass transport rate in the electro-crystallization can be readily manipulated through the control of deposition potential without changing the reactant concentration [5]. Although the electrodeposition of gold nanostructures has been studied [12,16], a number of differences are noted when compared. Since the preparation of gold nanostructures on screen printed carbon electrode (SPCE) in this study purposely for sensor applications, certain properties need further attention during the preparation of nanostructured gold coatings. It is important to produce high electrochemical active surface area with nano-sized crystals of gold coating on SPCE for glucose sensor, specifically.

In this study, gold nanostructures were deposited on SPCE by electrodeposition method using chronoamperometry (CA) mode at various deposition potentials. The prepared gold coatings were characterized for their surface morphology, elemental composition and crystallographic structure, phase content and crystallite size by FESEM, EDAX and XRD, respectively. Meanwhile, the electrochemical active surface area (ECSA) and electron transfer of gold coating were analyzed by cyclic voltammetry (CV).

2. EXPERIMENTAL

2.1 Materials

Tetrachloroauric (III) acid trihydrate ($HAuCl_4.3H_2O$) was purchased from Aldrich Co., Ltd; concentrated sulphuric acid (H_2SO_4), potassium ferrocyanide ($K_4[Fe(CN)_6]$) and potassium chloride (KCl) were purchased from Sigma-Aldrich. Screen printed carbon electrode (SPCE) with working electrode area of 0.126 cm^2 was obtained from Metrohm Sdn Bhd. In all the procedures, the solutions were prepared and diluted with ultra-pure water.

2.2 Preparation of Gold Nanostructures modified SPCE electrode

Gold nanostructures were directly electrodeposited on SPCE surface via potentiostatic method. An electrolyte solution for the deposition was prepared by dissolving 10 mM tetrachloroauric (III) acid ($HAuCl_4$) in 1.0 M sulphuric acid (H_2SO_4) at pH 2. A three-electrochemical cell was used for the deposition comprising of SPCE as the working electrode, a clean platinum as the counter electrode and a silver/silver chloride (Ag/AgCl) electrode as the reference electrode. Electrodeposition was performed using Autolab potentiostat (Aut302 FRA 2) interfaced with a PC running NOVA software. Initially, cyclic voltammetry (CV) procedure was performed by a single potential scan between +1.5 V to -1.0 V with scan rate of 100 mV/s in order to identify the right potential range for deposition of gold. After that, the chronoamperometry (CA) was employed to study the effect of different potentials on the formation of gold coatings on the SPCE surface. Based on cyclic voltammogram, four deposition potentials (i.e.: +1.0 V, +0.48 V, -0.3 V and -0.7 V) were chosen to investigate the effect of deposition potential on the formation of gold nanostructures coating on SPCE at a constant deposition time of 1200 s at room temperature.

2.3 Characterization of Gold nanostructures coating

The surface morphology and elemental composition of the prepared gold nanostructures on SPCE were characterized using Field Emission Scanning Electron Microscope (FESEM, Carl Zeiss SMT Supra 40VP) and Energy Dispersive X-Ray spectroscopy (EDAX), respectively. The crystallographic structure, phase content and crystallite size of gold nanostructures were characterized by X-ray Diffractometer (X'pert pro-MPD, PANalytical). The electrochemical active surface area (ECSA) of the deposited gold coatings was calculated from the area of voltammogram (i.e.: reduction area of gold nanostructures coating) by performing cyclic voltammetry (CV) analysis in 0.5 M sulphuric acid (H_2SO_4) solution. The electrochemical reactions (i.e.: reversibility and electron transfer ability) of the nanostructured gold electrodes were tested by cyclic voltammetry (CV) in 1mM $K_4[(Fe\ (CN)_6)]$ and 0.1 M KCl solution as supporting electrolyte.

3. RESULTS AND DISCUSSION

3.1 Cyclic Voltammetry Analysis

Initially, cyclic voltammetry (CV) analysis was carried out to investigate the deposition and dissolution processes of gold on screen printed carbon electrode (SPCE) surface. The CV analysis was performed in 10 mM tetrachloroauric (III) acid trihydrate ($HAuCl_4$) solution containing 1.0 M sulphuric acid (H_2SO_4) at pH 2 by scanning potential from +1.5 V to -1.0 V and switched back to +1.5 V at scan rate of 100 mV/s as shown in Figure 1. The forward scan exhibits the reduction of gold, inducing the deposition of gold particles onto SPCE surface. From the voltammogram, it can be seen that at the beginning of potential from +1.5 V to +1.1 V there was no current produced indicating no reaction occurred on the SPCE surface. Then, a small cathodic current peak appeared at potential of +1.0 V demonstrating a little nucleation of gold particles on the SPCE surface. However, a bigger cathodic current peak appeared at +0.48 V was ascribed to more nucleation as well as growth of gold on the SPCE surface.

Thereafter, the current started to decrease from +0.48 V to -0.15 V due to depletion of gold ions at the interface of the SPCE surface. Further scanning the potential to more negative value at -0.3 V resulted in a small current peak. At more negative potential of -0.4 V until -1.0 V, the current has increased drastically and this attributed to more evolution of hydrogen gas (H_2) simultaneously with the reduction of gold on the SPCE surface.

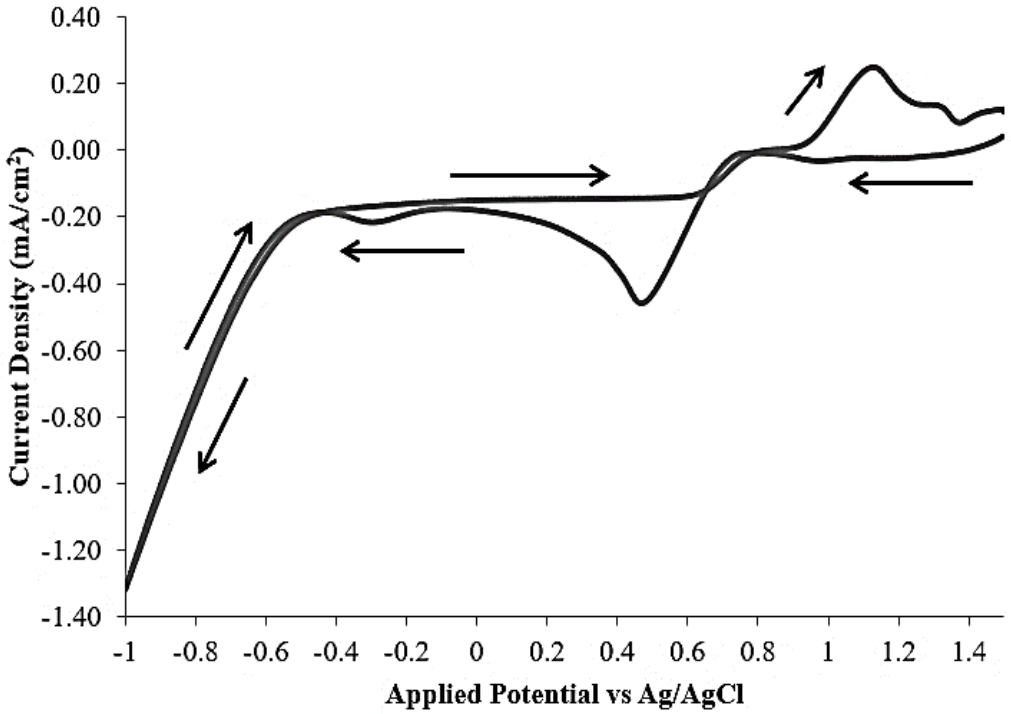

Figure 1. Cyclic Voltammogram of SPCE in 10 mM $HAuCl_4$ + 1.0 M H_2SO_4 (pH 2) at 25^{o}C. Scan rate: 100 mV/s. The arrows indicate the direction of cycle scan.

On the reverse scan, a crossover at -0.4 V was detected and it is attributed to the starting of reduction of hydrogen ion to hydrogen gas (Hydrogen Evolution Reaction, HER) as shown in Reaction 1.

$$2H^+ + 2e^- \rightarrow H_2 \quad (1)$$

Further scanning on positive potential, the cathodic current decreases and another current crossover occurred at +0.7 V. Previous study stated that this current crossover occurred due to nucleation and growth taking place with measurable rate known as the nucleation overpotential [17]. It is noteworthy that the current crossover occurred due to the consumption of $AuCl_4^-$ in the diffusion layer [18]. Whilst, the third current crossover occurred at +0.8 V is corresponding to the equilibrium of Au^{3+}/Au redox reaction. Due to the difference in deposition and dissolution potentials, a crossover occurs between the cathodic and anodic current traces [17,19]. At more positive potential (i.e.: +0.8 V until +1.5 V), one can observe the emergence of anodic current indicating the oxidation of Au to AuO.

3.2 Chronoamperometric Analysis

In order to study the effect of deposition potential on the formation of the gold nanostructures on SPCE surface, four different potentials were chosen based on CV as shown earlier in Figure 1 for the deposition process using Chronoamperometry (CA) method. Figure 2 shows the chronoamperometric curves for the deposition of gold on SPCE surface. It is noted that the deposition time was made constant to 1200 s for all deposition potentials. It can be seen that the current density has increased with increasing deposition potentials.

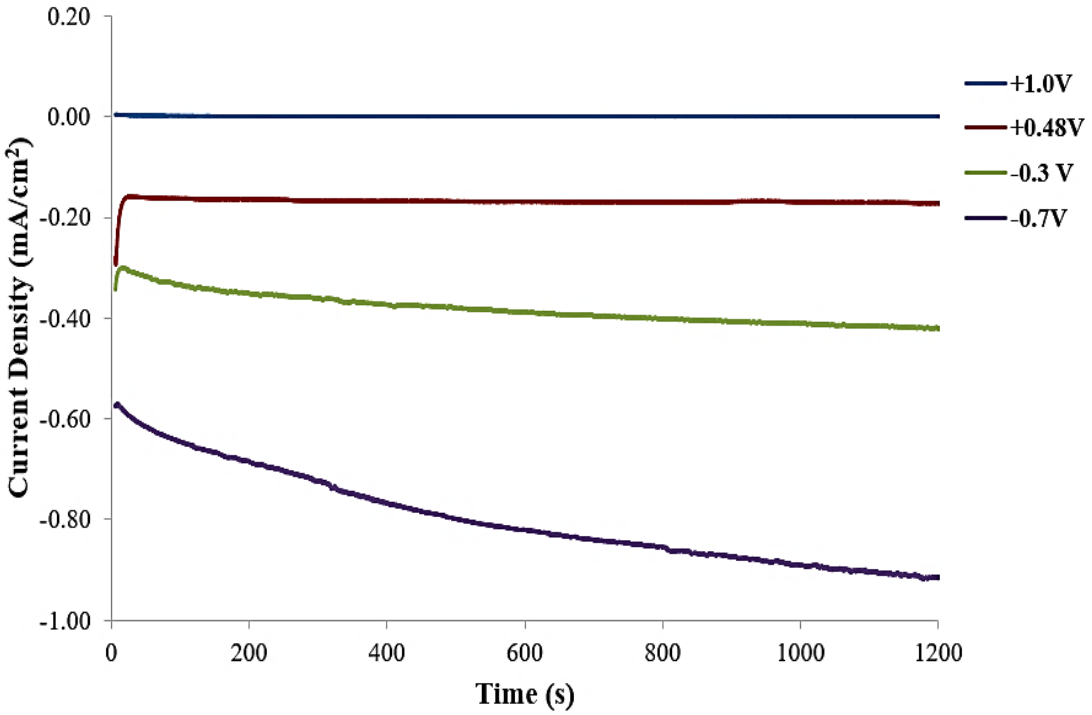

Figure 2. Chronoamperometric curves of electrodeposition of gold on SPCE surface by applying a constant potential of +1.0 V, +0.48 V, -0.3 V and -0.7 V for 1200 s.

At deposition potential of +1.0 V, the measured current density was very low at -0.015 mA and remain unchanged until 1200 s during the deposition, suggesting low charge transfer for the growth of gold on the SPCE surface. It is interesting to observe a smooth chronoamperometric curve is recorded for deposition potential at +0.48 V with a stable current density of -0.170 mA until1200 s. This indicates uniform a nucleation and growth of gold on the SPCE surface. At this potential range (i.e.: +1.0 V to +0.48 V) there are no bubbles formed on the SPCE surface signifying no interference from evolution of hydrogen gas. When the deposition potential was set at -0.3 V, the cathodic current density slightly decreased for the first 30 s but slowly increased thereafter indicating fast nucleation and growth of Au nucleus on the electrode surface. From 600 s to 1200 s, a few hydrogen gas bubbles were observed present at the SPCE surface showing that HER has already occurred at -0.3 V but with a slow formation rate.

When deposition potential was increased to a more negative value (i.e.: -0.7 V), the current density increased with increasing deposition time. This is due to a prominent side reaction of HER occurring at the electrode surface simultaneously with the deposition of gold. At this applied potential, a lot of hydrogen bubbles were vigorously formed on the electrode surface.

3.3 Characterization of Gold Coatings

The applied potential used for the deposition is an important factor in controlling the morphologies and structures of gold [20-21]. FESEM characterization was performed to investigate the effect of electrodeposition potential on the morphology of gold nanostructures. Figure 3 shows the surface morphologies of the gold nanostructures deposited on SPCE under different applied potentials for 1200 s from 10 mM $HAuCl_4$ solution.

Under deposition potential of +1.0 V (Fig. 3a), the as-prepared gold coating consists of small tetrahedral-like nanostructures that are dispersed on the SPCE surface with particle size less than 50 nm. However, the gold coating did not fully cover the SPCE surface due to low current flow during the deposition which limit the nucleation and growth of gold nanostructures. When the potential was applied at +0.48 V, the morphology of the gold has totally changed to quasi-spherical and facetted nanostructures (Fig. 3b) which covered the entire SPCE surface. Meanwhile, electrodeposition at -0.3 V resulted in some simple dendrite-like gold nanoclusters with several micrometres of stem structures (Fig. 3c). The growth of dendrite-like gold nanoclusters is due to far-equilibrium (diffusion-limited) conditions, as an example of sufficiently negative applied potential in electrodeposition [22-23]. At deposition potential of -0.7 V with the presence of hydrogen evolution reaction, a dense and rough with large micrometres of stems and feather-like branches of gold structures are formed on the SPCE as shown in Fig. 3d.

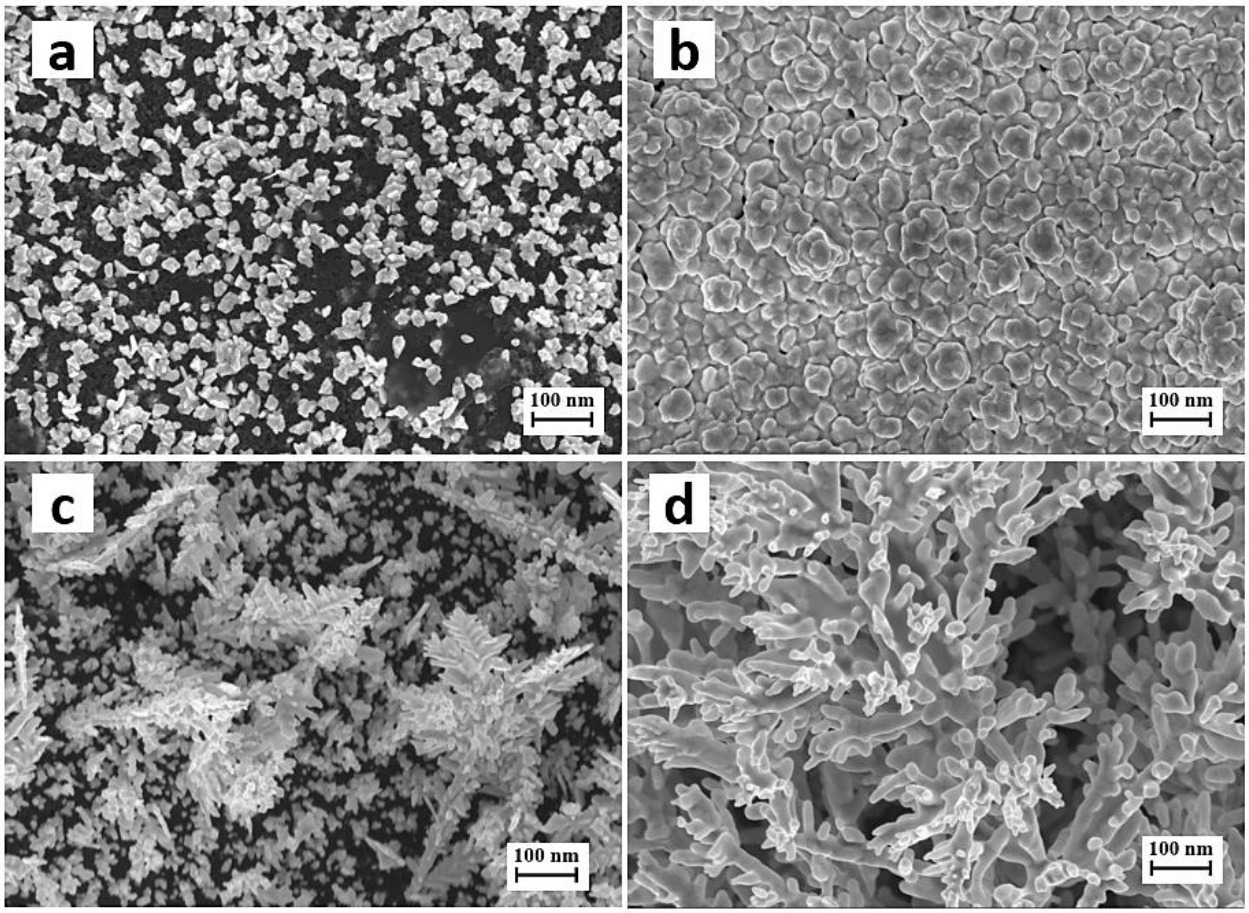

Figure 3. FESEM images of gold nanostructures prepared from 10 mM $HAuCl_4$ + 1.0 M H_2SO_4 (pH 2) at 25 ^{o}C for 1200 s at (a) +1.0 V, (b) +0.48 V, (c) -0.3 V and (d) -0.7 V. Magnification 20000x.

The elemental compositions of gold nanostructures coated on SPCE prepared at various deposition potentials are shown in Table 1. Analysis of the coating prepared at +1.0 V showed only 59.45 wt. % of Au present. The amount of carbon (C) detected was high at this deposition potential ascribed to low surface coverage of SPCE with Au nanostructures as shown by FESEM image in Fig. 3a. The Au amount was low due to a very low current flow during the deposition process. However, high amount of gold was detected with 99.68 wt.% for deposition at +0.48 V with low amount of oxide formed and the absence of C element suggested that the Au was fully deposited on the substrate's surface. Nevertheless, when deposition was carried out at -0.3 V and -0.7 V where the hydrogen evolution reaction (HER) was also occurring, the amount of Au slightly decreased to 96.61 wt.% and 95.64 wt.%, respectively. A small amount of C was also detected on both samples indicating incomplete surface coverage of SPCE with Au. This is because of the formation of H_2 bubbles at the SPCE surface blocking the deposition of gold. The remaining oxygen cannot be eluded as Au itself can be oxidized to AuO when exposed to environment.

Table 1. The elemental composition of gold nanostructures coating prepared at different deposition potentials

Deposition Potential (V)	Surface Composition (Weight (wt. %))		
	Au	O	C
+1.0	59.45	1.24	39.31
+0.48	99.68	0.32	ND
-0.3	96.61	1.24	2.15
-0.7	95.64	1.58	2.78

ND = Not Detected

XRD analysis was conducted on all gold coatings to identify the monocrystalline nature and crystallite sizes of the gold nanostructures formed. Based on the diffractograms as shown in Figure 4, only one diffraction peak corresponding to Au nanostructures (JCPDS 089-3697) was observed at deposition potential of +1.0 V at $2\theta = 38.4^{o}$ with (111) plane. Whilst, for gold coating deposited at +0.48 V, four Au diffraction peaks were detected (JCPDS 002-1095) at $2\theta = 38.5^{o}$, 44.7^{o}, 64.9^{o}, 77.6^{o} corresponding to (111), (200), (220) and (311), respectively. The diffractograms for gold coatings deposited at -0.3 V as well as -0.7 V exhibited similar diffraction peaks of gold nanostructures (JCPDS 089-3697) at 2θ and planes with 38.5^{o} (111), 45.2^{o} (20), 65^{o} (200) and 78.3^{o} (311). The XRD analysis demonstrated that all the gold coatings contain pure crystalline Au. The Bragg reflection peaks of Au clearly indicated that the gold coatings are cubic monocrystalline structure, which is consistent with the crystallite structure of Au.

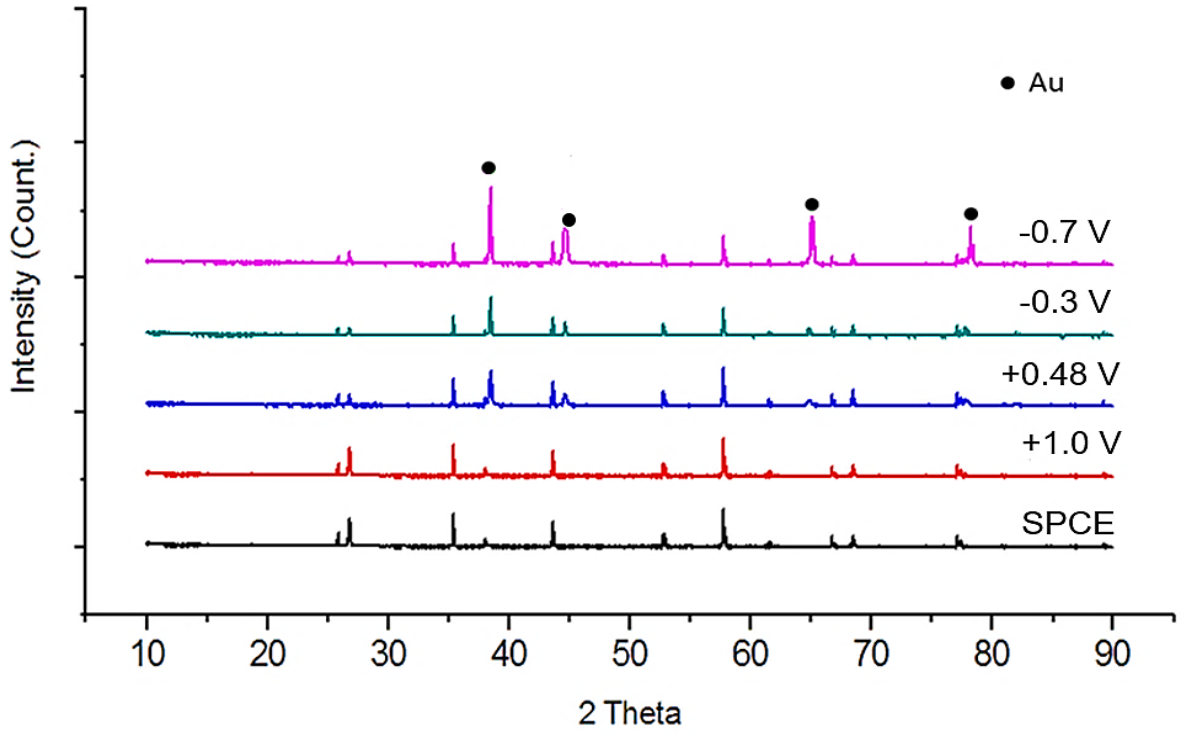

Figure 4. Representative XRD diffractograms of gold nanostructures synthesized by chronoamperometry from 10 mM $HAuCl_4$ + 1.0 M H_2SO_4 (pH 2) at 25^{o}C for 1200 s at +1.0 V, +0.48 V, -0.3 V and -0.7 V. XRD pattern of SPCE is also included as comparison.

The XRD patterns show a very high Bragg reflection peak corresponding to the (111) lattice plane. Thus, the crystallite size (D) for all gold coatings prepared at different deposition potentials was calculated based on the prominent plane (111) using the Scherer equation as in Equation 1:

$$D = 0.9\lambda/\beta \cos\theta \quad (1)$$

Where λ =X-ray radiation wavelength, β = full width at half maximum intensity and θ = Bragg angle in radian.

The calculated crystallite sizes of Au nanostructures at (111) lattice plane were 58.90 nm, 71.87 nm, 87.19 nm and 93.18 nm for +1.0 V, +0.48 V, -0.3 V and -0.7 V, respectively. The results show that increasing the deposition potential has resulted in the formation of bigger crystallite size of gold nanostructures.

3.4 Electrochemical Characteristics of gold nanostructures

For evaluating the electrochemical properties (i.e.: electrochemical active surface area) of gold nanostructures coatings deposited on SPCE, cyclic voltammetry (CV) was carried out using 0.5 M sulphuric acid (H_2SO_4) solution [27]. Figure 5 shows the cyclic voltammograms of bare SPCE and gold nanostructures coatings deposited on SPCE at different deposition potentials in 0.5 M H_2SO_4 solution.

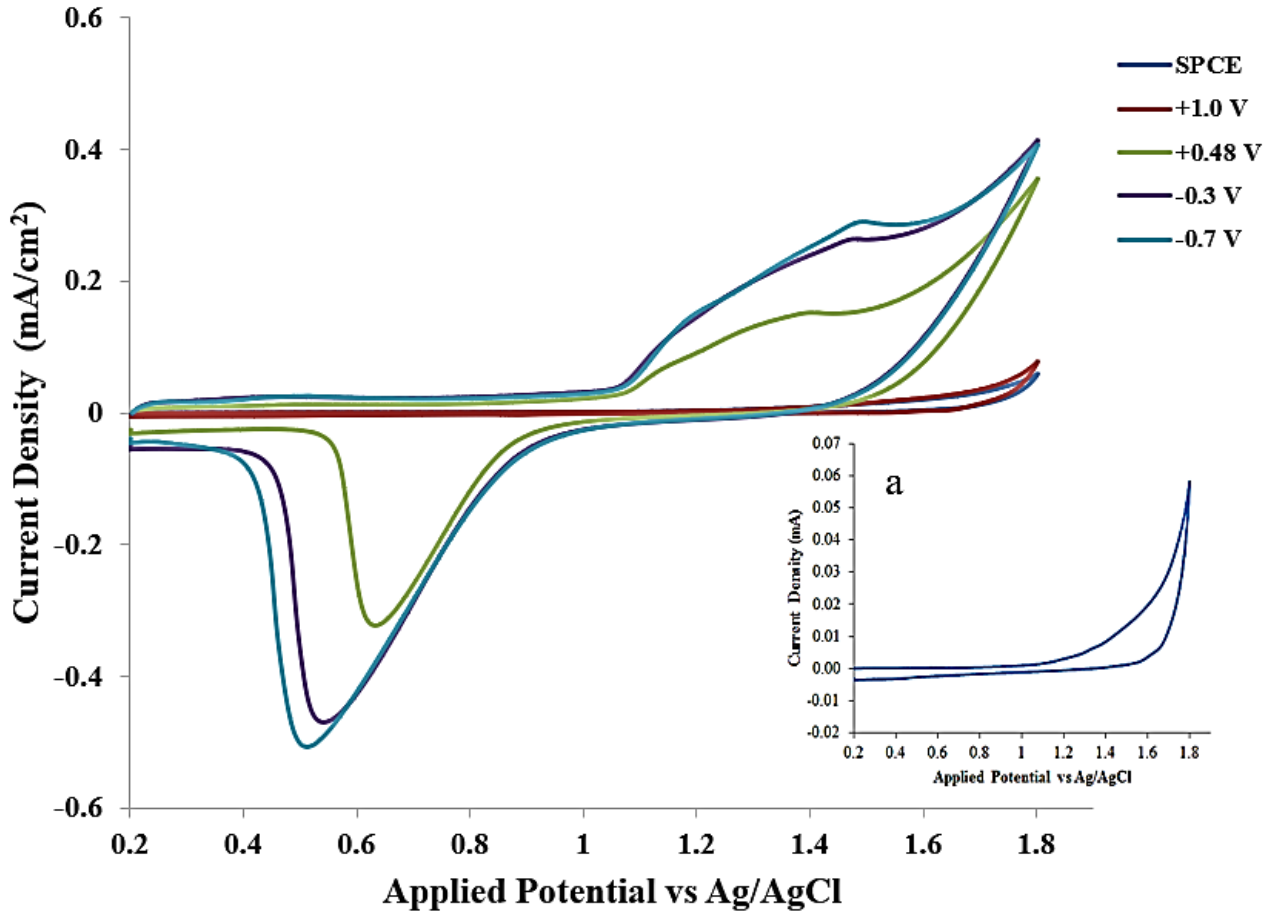

Figure 5. Cyclic voltammograms of nanostructured gold electrodes prepared at +1.0 V, +0.48 V, -0.3 V and -0.7 V in 0.5 M H_2SO_4 at scan rate 100 mV/s. Inset (a) CV of bare SPCE.

It is expected that the growth of gold nanostructures on SPCE surface would enhance the electrochemical active surface area (ECSA) of electrode which can increase the active sites, thereby the increase of active sites can improve the electrocatalytic performance [24-26]. The deposition potential has a significant effect on the electrochemical properties of modified electrode especially on active surface area used for the deposition [2, 26].

From the CV, anodic oxidation of gold started at +1.2 V and the cathodic reduction peak appeared at the range from +0.7 V to +0.75 V are attributed to the formation of gold oxide and a subsequent reduction of gold oxide to gold, respectively. Nevertheless, for bare SPCE, it is clearly observed that no reduction current response was recorded but only oxidation of water molecule to oxygen was observed (inset in Fig. 5a). Oxygen is assumed to be chemisorbed in a monoatomic layer of gold coating before the evolution of oxygen gas occurring at higher positive potential scanning with a one-to-one correspondence with the surface metal atoms [3,27].

The ECSA value of gold coatings can be calculated by evaluating the charge consumed during the reduction of gold oxide to gold in the negative scan, following the assumption that the monolayer of gold oxide was reduced and the reference charge density required to reduce the monolayer per unit of surface area (Q_{Os}) was 0.386 mC.cm^{-2} [18,28-29]. Thus, the estimation of ECSA can be determined using Equation 2.

$$\text{ECSA} = \frac{Q_O}{Q_{O\,s}} \qquad (2)$$

Where Q_O represents the surface oxide reduction (oxygen desorption) which corresponding to the integral area of cathodic peak (S) in CV diagram divided with the scan rate (v) (i.e.: $Q_O = \frac{S}{v}$).

Typically, the surface of a solid electrode is not smooth and its real area exceeds the geometric area and differs for different electrodes. The ratio between the ECSA and geometric area is called roughness factor, R_f.

The roughness factor (R_f) is calculated using Equation 3.

$$R_f = \frac{\text{Electrochemically active surface area (ECSA)}}{\text{Geometrical area of SPCE (0.126 cm}^2\text{)}} \qquad (3)$$

The ECSA and R_f values of all gold nanostructures deposited on SPCE at different deposition potentials are shown in Table 2. The researchers highlighted that the ECSA value will increase with increasing roughness of the coating surface [30]. According to previous results as reported by Sukeri and co-workers [31], the ECSA and Rf values of nanostructured gold deposited on SPCE were 1.513 cm^2 and 21.5, respectively. In this study, interesting to note that the ECSA and R_f of gold nanostructures prepared at -0.7 V are found to be much higher with 3.851 cm^2 and 30.5, respectively. These values were the highest as compared to other gold coatings deposited at different deposition potentials. These are correlated to its morphology as shown earlier in Figure 3d.

Table 2. The electrochemical surface area and roughness factor of gold coatings deposited at different deposition potentials.

Deposition Potential (V)	Electrochemical active surface area (ECSA) (cm^2)	Roughness factor (R_f)
+1.0	0.035	0.03
+0.48	1.684	13.4
-0.3	3.395	26.9
-0.7	3.851	30.5

The electron transfer characteristics of the surface of each gold electrode for redox couple of $Fe(CN)_6^{-3/-4}$ were studied and recorded by cyclic voltammetry (CV) in 1 mM Fe $(CN)_6^{-3/-4}$ dissolved in 0.1 M potassium chloride (KCl) as supporting solution as shown in Figure 6.

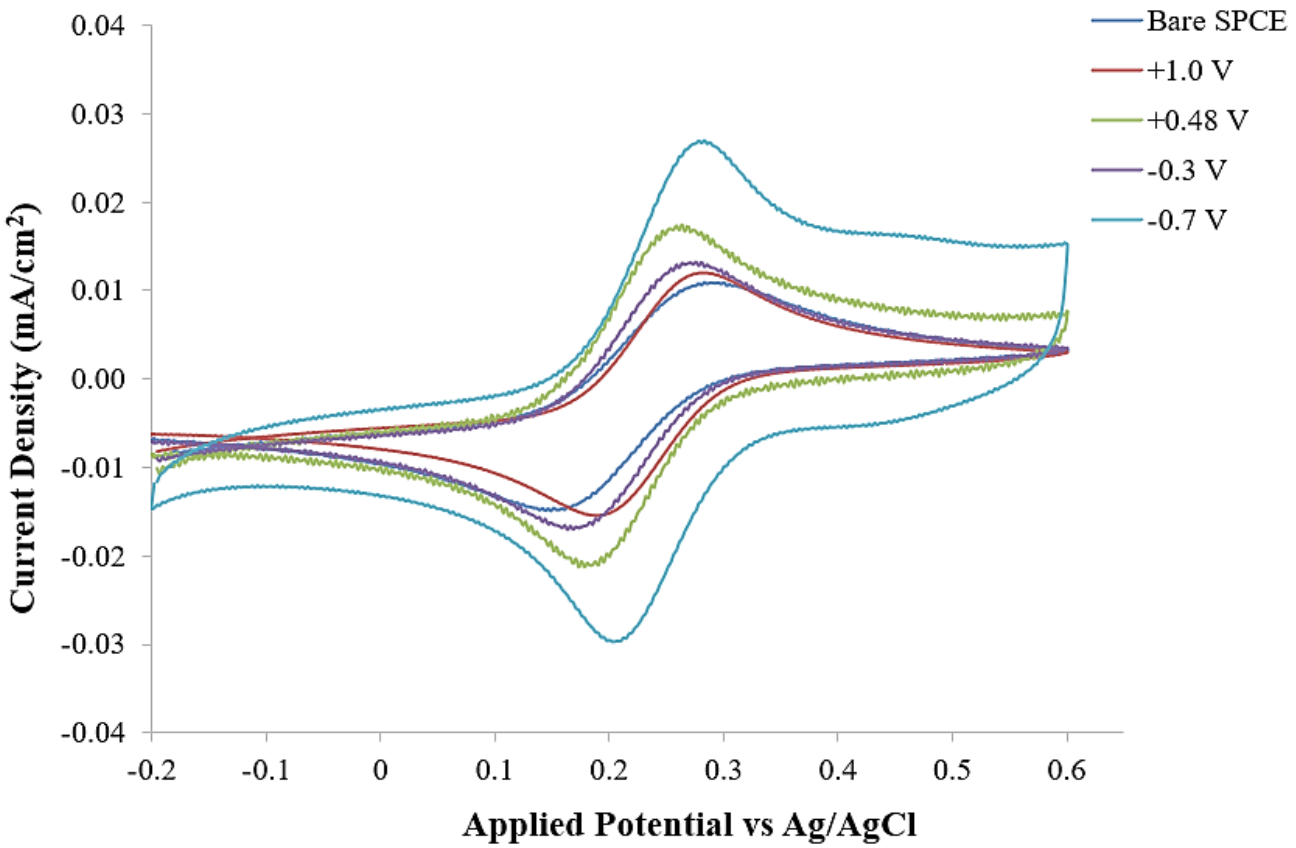

Figure 6. Cyclic voltammograms of bare SPCE and nanostructured gold coatings prepared at +1.0 V, +0.48 V, -0.3 V and -0.7 V in 1 mM $Fe(CN)_6^{-4}$ + 0.1 M KCl solution. Scanned at scan rate 100 mV/s.

Apparently, bare SPCE showed the lowest anodic and cathodic peak current density ratio (Ipa/Ipc) value for $Fe(CN)_6^{-3/-4}$ redox reaction with 0.75. However, upon modification of the SPCE surface with gold nanostructures, the redox current showed a step increase with small decrease in the potential difference. As seen in Figure 6, the Ipa/Ipc value was 0.80 for gold electrodes prepared at +1.0 V and +0.48 V and 0.90 for -0.3 V and -0.7 V. The most probable reason of the increase of current

density ratio values is due to the enhancement of electrochemical active surface area of SPCE electrode containing gold nanostructures, thus has increased the electrocatalytic activity for Fe $(CN)_6^{-3/-4}$ reaction and synergistic effect of the favorable conducting properties [32-33]. From these cyclic voltammograms, higher Ipa/Ipc values were determined for all nanostructured gold electrodes as compared to gold electrodes in the literature with only 0.66 [34]. The increment of Ipa/Ipc values has occurred upon modification of SPCE with gold nanostructures and this finding indicates that these gold nanostructures display high electrochemical active surface area along with an eased electron transfer rate. Thus, it can be concluded that the $Fe(CN)_6^{-3/-4}$ redox reaction on all gold samples was a quasi-reversible reaction.

Thereafter, the electrochemical study was extended to investigate the effect of scan rate on the voltammetric behavior of gold nanostructure. Figure 7 shows the cyclic voltammograms of nanostructured gold electrode prepared at -0.7 V in 0.1 M KCl containing 1 mM ferrocyanide scanned at various scan rates from 50 mV/s to 500 mV/s. It is noticeable from the cyclic voltammograms that each of the scan rate shows similar CV profiles where the redox peaks current densities (Ipa and Ipc) are enhanced as the scan rate increases. The peak potentials are slightly shifted to more positive potential for Epa and more negatively for Epc with increasing scan rates.

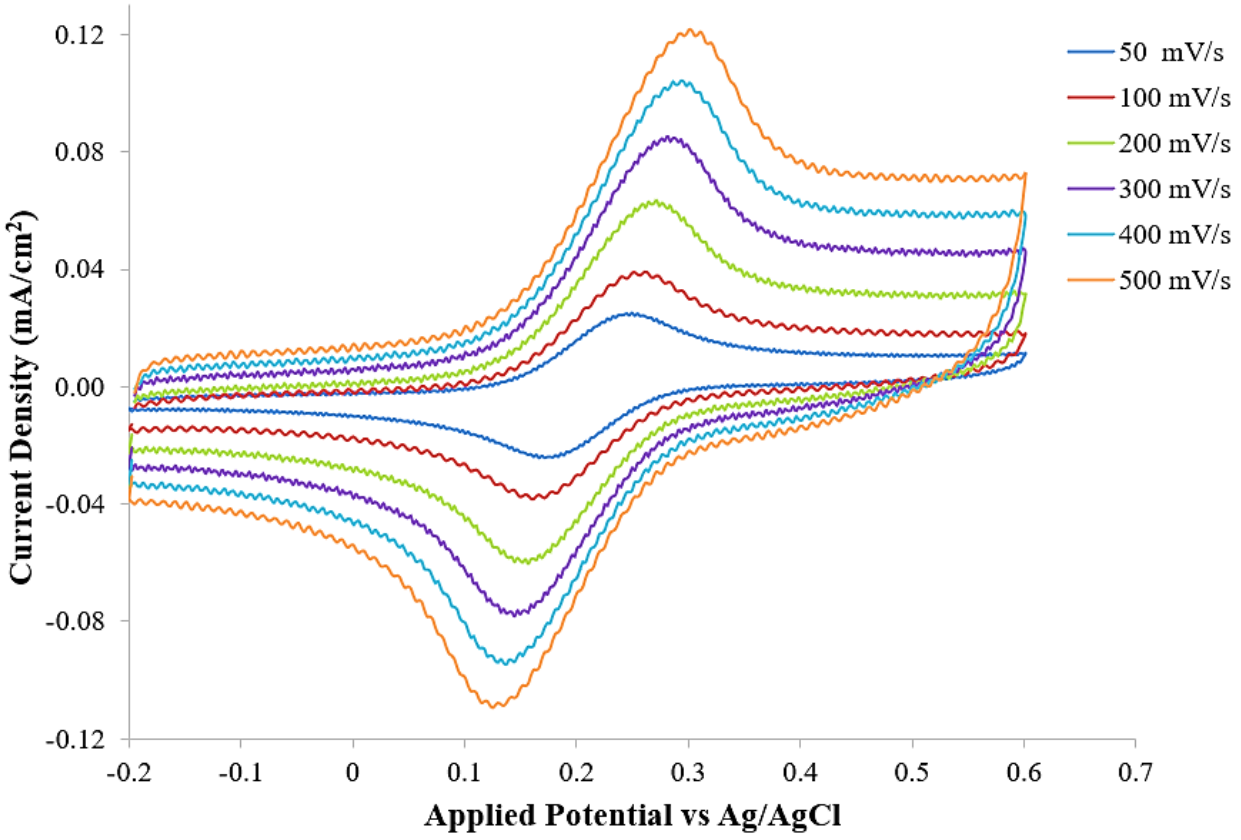

Figure 7. Cyclic voltammograms of nanostructured gold electrode prepared at -0.7 V in 1 mM $Fe(CN)_6^{-4}$ + 0.1 M KCl solution at different scan rates.

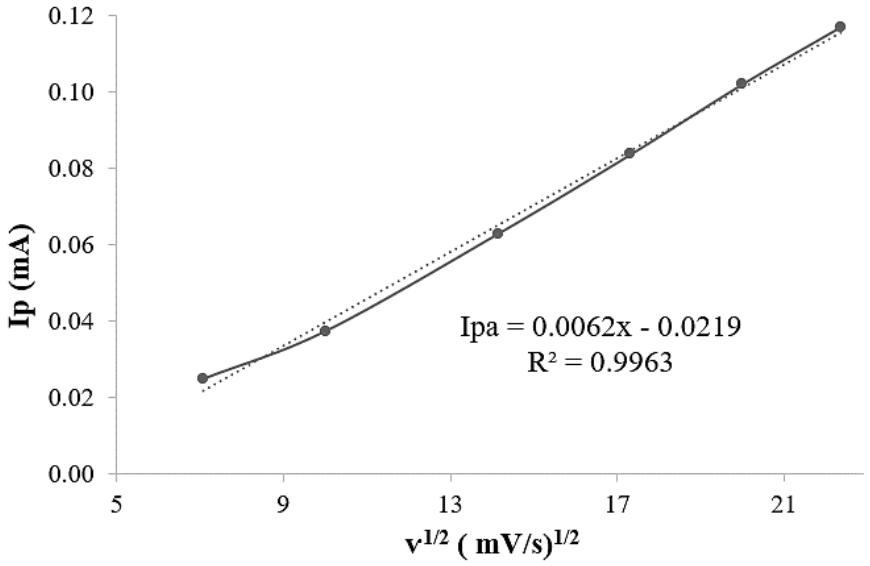

Figure 8. The fitting plot between Ipa and $v^{1/2}$ of gold coating deposited at -0.7 V in 1 mM $Fe(CN)_6^{-4}$ + 0.1 M KCl solution with different scan rates.

The electrochemical kinetic mechanism of $Fe(CN)_6^{-4}$ on gold surface was investigated by plotting the anodic peak current (Ipa) versus square root of the scan rate ($v^{1/2}$) as shown in Figure 8. It is evident that the plot of Ipa versus $v^{1/2}$ for gold coating deposited at -0.7 V exhibits an excellent linearity with high correlation coefficient of 0.9963, indicating that the Fe $(CN)_6^{-4}$ oxidation occurred on the gold coating electrode is a diffusion-controlled process.

4. CONCLUSION

Gold nanostructures were successfully deposited on the surface of SPCE using electrodeposition technique. Cyclic voltammetry and chronoamperometry methods were used to study the electrochemical deposition of gold nanostructures on the SPCE surface. It was shown that deposition potential has significantly affected the surface properties of gold nanostructures deposited on SPCE surface. The deposition potential has obviously influenced the morphology, elemental composition and crystallite size of the gold nanostructures. Different deposition potential used for the deposition has resulted in the formation of different surface morphology with different gold composition as well as different crystallite size. Through electrochemical performance analysis, the nanostructured gold coating produced at -0.7 V has the highest electrochemical active surface area (ECSA) and roughness factor with 3.851 cm^2 and 30.5, respectively. This coating gives the best electron transfer as compared to other gold coatings. The electrochemical kinetic mechanism $Fe(CN)_6^{-3/-4}$ on the nanostructured gold electrode prepared at -0.7 V was predominantly controlled by a linear diffusion. Therefore, this nanostructured gold electrode deposited on SPCE can further be used as sensing material for glucose detection in the near future.

ACKNOWLEDGEMENT
The work was financially supported by the Ministry of Education (Malaysia) through Fundamental Grant Scheme (FRGS) 600-RMI/FRGS 5/3 (094/2019) and Faculty of Applied Sciences, Universiti Teknologi MARA (UiTM) Shah Alam, Selangor for the facilities provided.

References

1. K. U. Lee, J. Y. Byun, H. J. Shin and S. H. Kim, *J. Alloys Compd.,* 779 (2019) 74.
2. G. Chang, H. Shu, K. Ji, M. Oyama, X. Liu and Y. He, *Appl. Surf. Sci.,* 288 (2014) 524.
3. Zabihollahpoor, M. Rahimnejad, G. Najafpour and A. A. Moghadamnia, *J. Electroanal. Chem.,* 835 (2019) 281.
4. T. Liang, X. Guo, J. Wang, Y. Wei, D. Zhang and S. Kong, *Mater. Lett.,* 254 (2019) 28.
5. N. Wongkaew, M. Simsek, C. Grieshe and A. J. Baeumner, *Chem. Rev.,* 119 (1) (2018) 120.
6. C.H. Voon and S.T. Sam, Physical surface modification on the biosensing surface. *Nanobiosensors for Biomolecular Targetting* (2019).
7. M.S. Seehra and A.D. Bristow, Introductory chapter: Overview of the properties and applications of noble and precious metals. *Noble and Precious Metals-Properties, Nanoscale Effects and Applications* (2019).
8. N. X. Viet, M. Chikae, Y. Ukita and Y. Takamura, *Int. J. Electrochem. Sci*.,13 (2018) 8633.
9. Mirzaei, J. H. Kim, H. W. Kim and S. S. Kim, *Sens. Actuators, B.,* 258 (2018) 270.
10. M. Shumba and T. Nyokong, *Electroanalysis,* 28 (7) (2016) 1278.
11. D. Dechtrirat, P. Yingyuad, P. Prajongtat, L. Chuenchom, C. Sripachuabwong, A. Tuantranont and I. M. Tang, *Microchim. Acta,* 185 (2018) 1.
12. S. Yang, Y. Zheng, X. Zhang, S. Ding, L. Li and W. Zha, *J. Solid State Electrochem.,* 20 (7) (2016) 2037.
13. G. Hughes, K. Westmacott, K. Honeychurch, A. Crew, R. Pemberton and J.Hart, *Biosensors,* 6 (4) (2016) 50.
14. N. Wongkaew, M. Simsek, C. Griesche and A. J. Baeumner, *Chem. Rev.,* 119 (1) (2018) 120.
15. M. M. Collinson, *ISRN Analy. Chem.*, 2013 (2013) 1.
16. J. Bhattaria, D. Neupane, B. Nepal, V. Mikhaylov, A. Demchenko and K. Stine, *Nanomaterials,* 8 (3) (2018) 171.
17. N. N. C. Isa. Y. Mohd, M.H.M Zaki and S.A.S. Mohamad, *Int. J. Electrochem. Sci.*, 12 (2017) 6010
18. T. Hezard, K. Fajerwerg, D. Evrard, V. Collière, P. Behra and P. Gross, *J. Electroanal. Chem.,* 664 (2012) 46.
19. A. Mallik and B.C. Ray, Int. J. Electrochem., 2011 (2011) 1.
20. H. Shu, L. Cao, G. Chang, H. He, Y. Zhang and Y. He, *Electrochim. Acta,* 132 (2014) 524.
21. J. Hovancová, I. Šišoláková, P. Vanýsek, R. Oriňaková, I. Shepa, M. Vojtko and A. Oriňak, *Electroanalysis,* 31 (2019) 1680.
22. E. Rafatmah and B. Hemmateenejad, *Sens. Actuators, B,* 304 (2020) 127335.
23. K. Fukami, S. Nakanishi, H. Yamasaki, T. Tada, K. Sonoda, N. Kamikawa, N. Tsuji, H. Sakaguchi and Y. Nakato, *J. Phys. Chem, C*, 111(3) (2007)1150.
24. K. Yuan, Z. Xiao, H. Yang, S. Yin, J. Zhang, Z. Yang and Y. Ding, *Nanoscale,* 12 (2020) 4314.
25. Sukeri, A. Arjunan, A and M. Bertotti, *Electrochem. Commun.,* 110 (2020) 106622.
26. Zabihollahpoor, M. Rahimnejad, G. Najafpour and A. A. Moghadamnia, *J. Electroanal. Chem.,* 835 (2019) 281.
27. T. Hezard, K. Fajerwerg, D. Evrard, V. Collière, P. Behra, P.Gros, *J. Electroanal. Chem.*, 664 (2012) 46.
28. S. Trasatti and O.A Petrii, *J. Electroanal. Chem.,* 327 (1-20) (1992) 353.
29. S. Trasatti and O.A Petrii, *Pure Appl. Chem.*, 63 (5) (1991) 711.

30. M. Vafaiee, M. Vossoughi, R. Mohammadpour and P. Sasanpour, *Sci. Rep.*, *9*(1) (2019) 1.
31. A. Sukeri, L. P. H. Saravia and M. Bertotti, *Phys. Chem. Chem. Phys.*, *17*(43) (2015) 28510.
32. A.S. Rajpurohit, N.S. Punde and A.K. Srivastava, *New J. Chem*., 43(42) (2019) 16572.
33. P. Kanyong, S. Rawlinson and J. Davis, *Microchim. Acta*, 183(8) (2016) 2361.
34. N.X. Viet and Y. Takamura, *VNU J. Sci.: Nat. Sci. Technol*., 34(4) (2016) 83.